Journal of Quantitative Spectroscopy & Radiative Transfer 132 (2014) 22–27

Contents lists available at ScienceDirect

Journal of Quantitative Spectroscopy & Radiative Transfer

journal homepage: www.elsevier.com/locate/jqsrt

Effects of randomness and inclination on the optical properties of multi-walled carbon nanotube arrays

Hua Bao [a,b], Bhagirath Duvvuri [a], Minhan Lou [b], Xiulin Ruan [a,*]

[a] School of Mechanical Engineering and Birck Nanotechnology Center, Purdue University, West Lafayette, IN 47907, United States
[b] University of Michigan-Shanghai Jiao Tong University Joint Institute, Shanghai Jiao Tong University, Shanghai 200240, China

ARTICLE INFO

Article history:
Received 30 August 2012
Received in revised form
31 March 2013
Accepted 14 April 2013
Available online 23 April 2013

Keywords:
Carbon nanotube
Array
Optical
Randomness
Inclination

ABSTRACT

The optical properties of multi-walled carbon nanotube arrays are investigated using the finite-difference time-domain method, focusing on the effects of various structural randomness, including random position, diameter, length, and orientation. It is found that the arrays with random position, diameter, length, and small inclination angle have quite small absorption enhancement compared to the ordered arrays. The reflection spectra of the arrays with random position, diameter, and small inclination angles are almost identical to the ordered array, but large reflection suppression is seen in vertical arrays with random length. For oblique arrays, the absorptance increases with inclination angle for S-polarized light, but weakly depends on inclination angle for P-polarized light. By comparing the inclined arrays with different volume fractions, the reflectance is found to be largely determined by the local volume fraction of the top surface of carbon nanotube arrays.

1. Introduction

Carbon nanotubes (CNTs) have attracted considerable interest since their discovery in 1991 [1], because of their unusual electrical, mechanical, thermal, and optical properties. Optical properties of CNT arrays are especially interesting as CNTs are strongly anisotropic [2,3] and highly absorbing in the visible and infrared regions. Low density arrays of vertical CNTs have low effective index of refraction as well as numerous nanocavities that can effectively trap light, making them superior light absorbers [4–6]. For example, Yang et al. have reported multi-walled (MW) CNT arrays with reflectance as small as 0.045% in the visible range [4]. Wang et al. have shown that the optical reflectance of CNT array is about 0.5%, and can be either highly diffuse or specular, depending on the details of fabrication process [7]. Such high absorbing materials can be potentially useful in optical applications, such as radiometric temperature measurements [8] and fast-switching blackbody sources [9].

There have also been many theoretical investigations on the optical properties of CNT arrays. Calculations based on the density-functional theory have shown that the optical properties of small single-walled (SW) CNTs are strongly dependent on the chirality of each individual CNT [10]. However, when the CNTs are arranged in an array manner, the array usually contains CNTs with many different chiralities [11]. On the other hand, a single multi-walled (MW) CNT is composed of multiple concentric SWCNTs. Therefore, in most theoretical analysis, CNT arrays (regardless SW or MW) have been treated as an effective medium that contains many rolls of graphite. Some numerical electromagnetic calculations have also been carried out. For example, Lidorikis et al. used the finite-difference time-domain (FDTD) calculations for infinitely long MWCNT arrays with irradiation incident from one side of the array [12]. They predicted the CNT arrays to be good absorbers in the visible band and photonic crystals in ultraviolet band. In our earlier work, FDTD simulations are employed to calculate the optical properties of CNT arrays, with light incidence from the top [13]. We have demonstrated that the effective medium

* Corresponding author.
E-mail address: ruan@purdue.edu (X. Ruan).

0022-4073/$ - see front matter © 2013 Elsevier Ltd. All rights reserved.
http://dx.doi.org/10.1016/j.jqsrt.2013.04.015

theory cannot fully capture the wave effect so that the prediction from such theory is not accurate enough [13]. It has also been shown that such arrays are nearly perfect absorbers, which is qualitatively consistent with the experimental results [13]. Quantitative comparison is still a challenge because structural randomness is inherent to any CNT array fabrication process, and the effects have not been included in previous theoretical studies. It becomes essential to uncover whether structural randomness will deteriorate the optical reflection or absorption. Recent investigations on silicon nanowire arrays show that small randomness such as random position, diameter, and length can greatly enhance the optical absorption of the arrays [14]. Compared to silicon, MWCNTs are anisotropic in their optical properties and are much more absorbing in nature, and the effects of structural randomness may show different features.

In this study, the effects of various structural randomness for CNT arrays, i.e., random position, diameter, length, and orientation, are investigated systematically using the FDTD method. The aligned CNTs with different inclination angles up to 60° are also studied. The results are compared with the optical properties of those ordered vertical arrays.

2. Simulation details

The different structures studied in this work are illustrated in Fig. 1(a). The ordered array contains 16 CNTs with 40 nm diameter and 1500 nm length. For all the simulations with structural randomness or CNT inclination, we choose a similar structure which contains 16 individual CNTs. No substrate is placed below the array, so we are actually investigating a film that contains an array of CNTs. The dielectric function of CNTs is obtained from an averaging of the dielectric function of graphite, as in our previous work [13]. The various random arrays are generated so that they have comparable volume fraction with the ordered array, and the details will be provided in subsequent discussions.

Fig. 1(b) is an illustration of the vertical cross section of the simulation domain. The 3D simulation domain is a tetragonal shape of 400×400 nm in the xy plane, and 3100 nm in the z direction. Periodic boundary condition is applied in the x and y directions and the perfectly matched layer (PML) is used to truncate the z direction. A Gaussian source is placed at 1500 nm above the upper surfaces of the arrays. Two power monitors placed above and below the array are used to measure the transmitted and reflected flux values which are then normalized by the source power to obtain the reflectance and transmittance spectra. The absorptance spectra are then calculated using $A = 1 - T - R$, where T and R are the transmittance and reflectance from the simulation, respectively. Such a simulation setup is commonly used to model plane waves incident on a structure [13,15,16]. For all cases the reflectance and transmittance are calculated for 100 different wavelengths between 400 and 850 nm which cover the entire visible spectrum. All the simulations are performed with Lumerical FDTD solutions package. Automatic adaptive mesh with the highest possible accuracy is used for spatial discretization of the simulation domain.

Applying periodic boundary condition to this domain will generate pseudo-random configurations. These configurations are then used in the simulations to find out their optical properties. To ensure that our pseudo-random structures can capture the essential physics of real structural randomness, we have tested larger simulation domains with 800×800 nm or 1600×1600 nm size which contain 64 or 256 CNTs for the array with random position, and the results are similar. Also, ten randomly generated configurations are sampled for each types of randomness, and the transmittance and reflectance values are the average of the ten configurations.

3. Results and discussion

3.1. Effects of random position, diameter, and length

To generate CNT arrays with random position, the xy plane of the simulation domain is divided into sixteen 100×100 nm cells. One CNT with 40 nm diameter and 1500 nm length is

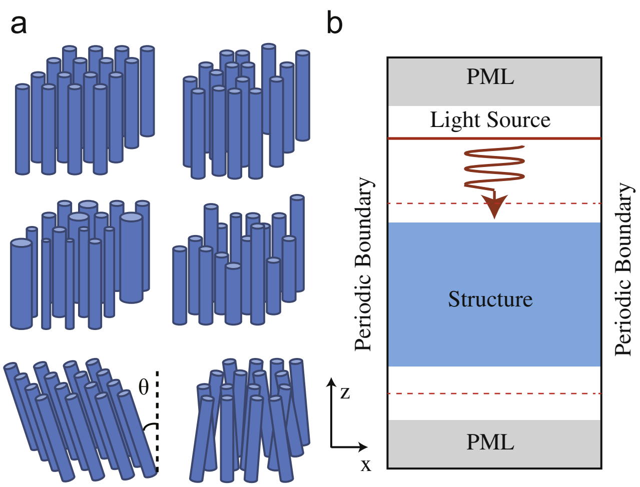

Fig. 1. (a) The various CNT arrays studied in this work, including ordered array, random position, random diameter, random length, oblique array, and random small inclination angle. (b) A cross section of the simulation setup. Periodic boundary conditions are applied at x and y directions. Two dashed curves indicate the flux monitors to calculate the reflected and transmitted flux.

randomly placed into each cell. For the random diameter array, the axis of the CNTs is placed at the center of each cell, while the diameter is a randomly generated number from 30 to 50 nm. For the random length array, the positions of the CNTs are kept ordered, while the lengths of the CNTs are selected as random numbers between 1000 and 2000 nm, such that the average length of the overall array is still 1500 nm. For different types of randomness, the distribution function is uniform in the allowed range. Note that the CNTs are kept vertically aligned for these three cases. The reflectance and absorptance spectra from 400 to 850 nm are calculated and compared with those of the ordered array, as shown in Fig. 2.

The predicted reflectance values of the ordered, random position, and random diameter arrays are around 0.2%, which is of the same order of magnitude as some experimental results reported in literature [7]. The reflectance values are all quite small, owing to the small real part of the dielectric function of CNT and the vertically aligned array structure. The magnitude of reflectance of the different arrays is almost identical except the random length one. There are some evident oscillations with respect to frequency, and the reflection maxima occur at approximately 726, 589, 499, and 430 nm. Such oscillations of reflectance spectra are commonly seen in thin film materials and are due to the Fabry–Perot effect (interference of the reflected waves at the top and bottom interfaces). For thin films with normal incidence, a reflection peak generally can be observed when

$$2nd = m\lambda, \tag{1}$$

where n is the refractive index, d is the thickness of the thin film, m is an integer, and λ is the wavelength in vacuum. An estimation based on the effective medium theory for vertical CNT arrays [13] gives an effective refractive index of the CNT array along the axial direction (real part) about 1.26 in the visible light regime. For a thin film of refractive index 1.26 and 1500 nm thickness, the peak wavelengths corresponding to m=5,6,7,8 are 756, 630, 540, and 472 nm, respectively. These are very close to the reflectance peaks in our numerical simulation. Therefore, the oscillations can be attributed to the Fabry–Perot effect, as what occurs in a thin film. The existence of this interference indicates that light does not "see" much of the nanostructures inside the array. They propagates almost like a plane wave, while only a small fraction is diffracted or scattered.

In comparison, the reflectance of random length array is much smaller. It also has little oscillation, since light is reflected from a rough surface at nanoscale and the interference effect is not significant. The further suppression of reflectance in the random length array can be explained by the further reduction of the dielectric contrast at the air–CNT array interface. This is the idea behind having a dual diameter array [17] or nano cone array [18] to create a gradient in the refractive index. In most fabrication processes the length will have a spread [19], and such a property of random length arrays is actually beneficial to further reduce the reflection and achieve even darker materials.

The absorptance values are in the range of 55–90%, depending on the wavelength. The absorptance decreases when the wavelength is longer for all cases, primarily due to the smaller imaginary part of CNT dielectric function at longer wavelength. Note that since our CNTs are very short, one should not make a direct quantitative comparison between the absorptance calculated here and the near unity absorptance in some experiments [4,5] where the CNTs are as long as a few hundred microns. But since the 1500 nm can absorb more than 55% of the incident light, one can see that the CNTs are quite absorptive. The arrays of a few hundred microns in the experiment can easily absorb all the incident light. On the other hand, by making a comparison of the absorptance of ordered and random arrays, we find that all the different types of random arrays only have slightly larger absorptance than the ordered array. Similar absorption enhancement compared to ordered array is also demonstrated in silicon nanowire arrays with random position or diameter, and can be explained by the enhanced optical scattering and field

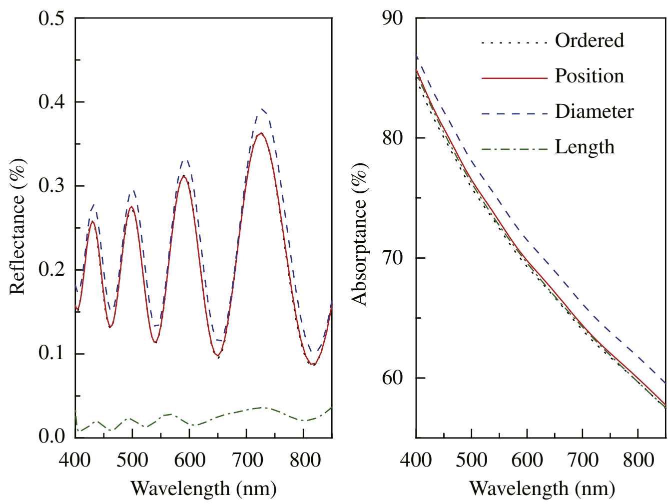

Fig. 2. The optical reflectance and absorptance of ordered CNT array and the arrays with random position, diameter, and length.

localization when randomness is induced [14]. The difference is that random position can enhance the absorption up to 20% and the random diameter can enhance the absorption up to 100% in silicon nanowire array. In CNT array, however, random position or length has almost negligible reflection enhancement. Even the random diameter arrays merely have an average enhancement of 2–4%. This difference can be attributed to the different material properties of CNT and silicon. While silicon has large refractive index and small attenuation coefficient in the visible regime (except very short wavelength), CNTs have small refractive index and high extinction index. The small refractive index makes the diffraction at the top surface of the CNT array to be relatively weak, so light is still propagating parallel to the CNT axis. Thus the structural randomness on the *xy* plane does not have an important effect on the light propagation. Also, the high extinction index of CNT makes the array very absorptive even without structural randomness. For both reasons, the absorption enhancement contributed by randomness is not as significant as the silicon arrays.

3.2. Effects of random small inclination

To investigate the effect of inclination angle on the optical properties of CNT arrays, we first consider small random inclination angles. The CNTs in a 4×4 array are randomly deviated within 5° from the *z* direction. The calculated reflectance and absorptance are shown in Fig. 3, together with the absorptance and reflectance of aligned CNTs with 5° and 10° inclination angles (as shown in Fig. 1(e)). The randomly inclined CNTs almost show the same reflectance as the ordered and 5° or 10° inclined array. The vertical array has smaller absorptance compared to 5° and 10° inclined array. Interestingly, the absorptance of randomly inclined array is larger than 5° inclined array and similar to the 10° inclined array. Since each individual CNT has inclination angle smaller than 5°, the small enhancement is related to the effect of randomness. However, the overall absorption enhancement of the small inclination angle is only a few percent compared to the vertically aligned array. Therefore, small random inclination angle does not have any significant effect on the optical properties of CNT arrays.

3.3. Effects of large inclination angle

For CNT arrays with large oblique angles, ideally we should study randomly oriented CNT mats, as we did for the random small inclined arrays. However, it is practically difficult to generate such structures without overlap of CNTs. Therefore we studied the aligned ones in this case. Note that we have previously considered the effect of oblique incidence on a vertical array [13], but the normal incidence on an oblique array is a different case. Because of the anisotropic nature of the CNTs we can expect different absorption properties for different CNT orientation angles. For oblique orientation we need to consider the polarization of incident light. Here we define that S polarization refers to the magnetic field vector being perpendicular to the CNT axis, while in the P polarization case the electric field vector is perpendicular to the axis of CNT. In this simulation the CNTs are obliquely oriented and the inclination angles vary from 0° to 60°. Here we have considered two cases of inclined arrays, as shown in the inset of Fig. 4. In the first case, the length of individual CNTs is kept constant so that the projected length on the incident direction is shorter at larger incident angle. As a result, the volume fraction is larger when the incident angle increases. In the second case, the volume fraction and projected length on the incident direction are kept constant, while the length of individual CNT increases and diameter decreases with increasing inclination angle.

The calculated absorptance and reflectance for different inclination angles are shown in Fig. 4. Here we only plotted two representative incident wavelengths of 400 and 700 nm. The angular dependence of reflection and absorption has similar features for all other wavelengths in the regime considered. For the oblique arrays that have constant volume fraction (denoted by "H" in Fig. 4), both

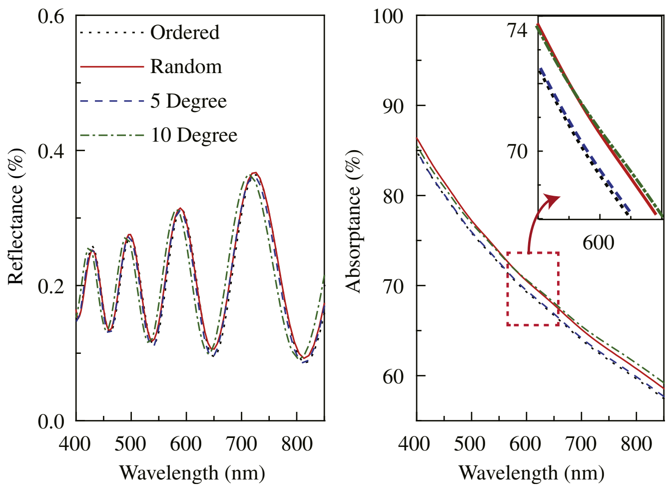

Fig. 3. The optical reflectance and absorptance of ordered array and the array with small random inclination angle. Also shown are the values for aligned arrays with 5° and 10° inclination angle.

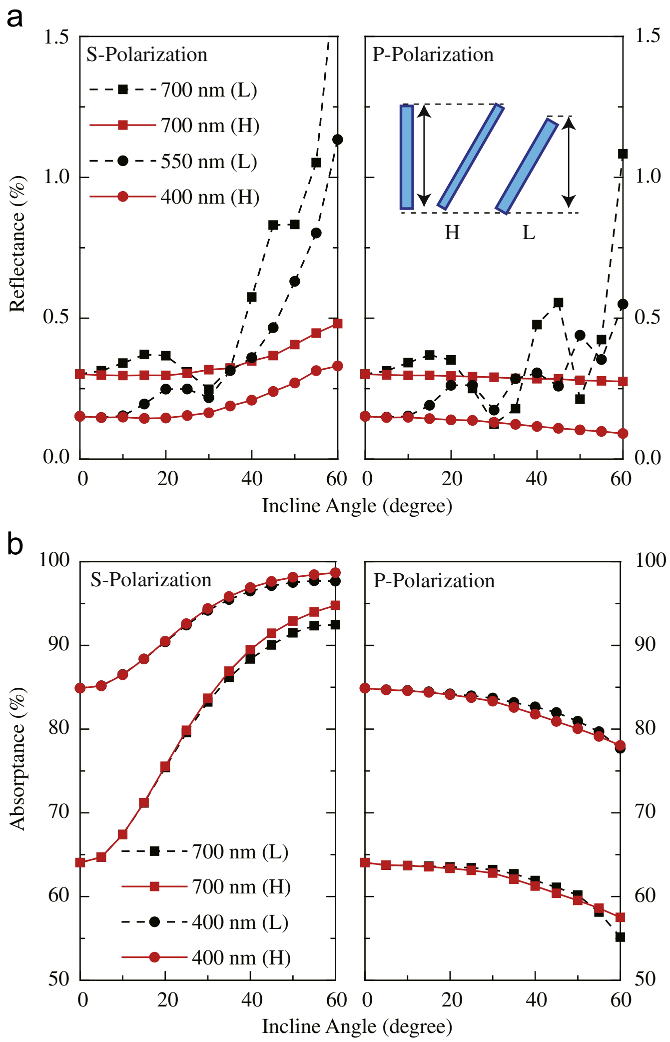

Fig. 4. The reflectance and absorptance of inclined arrays for 400 and 700 nm light at different inclination angles. Inset: "L" denotes the case that the length of individual CNTs is kept constant and "H" indicates that the projected length and volume fraction are kept constant. (a) Reflectance. (b) Absorptance.

absorptance and reflectance show quite distinct inclination dependence. For S-polarization, both absorptance and reflectance increase as the inclination angle becomes larger, while for P-polarization both absorptance and reflectance slightly decrease as the inclination angle increases. The angular dependence for S polarization is due to the strong anisotropy of CNTs. Both the real and imaginary parts of dielectric function when electric field parallel to the tube axis is much larger than those when electric field is perpendicular to the tube axis. As the inclination angle becomes larger, the dielectric function along the axial direction will become more important for the S-polarized incident light. Therefore, both the reflection and absorption become larger as the inclination angle increases. For the P-polarization, in contrast, the electric field of incident light is always perpendicular to the tube axis. Both the reflection and absorption are still contributed by the dielectric function perpendicular to the tube axis. Therefore, the optical reflection and absorption have quite small dependence on the inclination angle for P-polarized light. It should also be noted that as the inclination angle becomes larger, the reflectance value does not show a significant increase. Therefore, inclination without varying volume fraction will not result in a significant change of reflectance.

For the arrays with constant CNT length, the absorptance is similar to the constant volume fraction array. The same argument as the constant volume fraction array can be applied to explain such an angular dependence. Even though the volume fraction is larger for larger inclination angle which generally results in absorption enhancement, this effect is actually offset by the decrease of height in the incident direction. The reflectance spectra, however, have quite different angular dependences. First, it does not monotonically increase or decrease with the oblique angle. This has to do with the Fabry–Perot resonance effect, as seen in Fig. 2. As the inclination angle becomes larger, the projected length along the incident direction becomes smaller. For a particular wavelength, different inclination angles correspond to different phase differences for the light reflected at the frontal and back surface. For some angles the interference is constructive but for others they are not. More importantly, the overall reflectance increases more rapidly at larger inclination angle for both polarizations. This is due to the fact that as the inclination angle is larger, the volume fraction also increases accordingly from 12.5% (vertical) to 25% (60°), which leads to more light being reflected. It should be noticed that when the inclination angle is 60°, the reflectance is more than 1%, which is comparable to some experimental observations [6]. Although their arrays are largely vertically aligned, it still can be seen from the SEM images that some CNTs have large oblique angles near the top surface.

4. Further discussions

Potential applications of CNT arrays include extremely dark material, which requires both large absorption and small reflection. Our simulation results clearly show that for different types of randomness and obliqueness, the CNTs arrays have quite large absorption. For the arrays with 12.5% volume fraction, the 1500 nm CNTs can already absorb more than 50% of the incoming radiation. In experiments CNT arrays generally have smaller volume fraction, but the length can be a few hundred microns, which is sufficient to absorb all the light that enters the array. Therefore, to realize the best blackbody absorbers, the major task is to minimize the reflectance. Although it is practically difficult to model CNT arrays with such a length, the short CNT array in our simulation can be a mimic of the very top layer of long CNT arrays. The Fabry–Perot resonance will of course not be seen in experiments, but the order of magnitude of reflectance should be comparable to the experimental value. The existing experimental data of the reflectance spectra of vertical CNT arrays are quite different, ranging from 0.045% [4] to about 1% [6]. Our calculation results show that this range can indeed be achieved by CNT arrays with large inclination angles. By comparing the reflectance spectra of two different types of oblique arrays, we notice that only when the inclination of CNT causes the increment of local volume fraction, the reflectance increases. Therefore, the most important factor for the further reduction of reflection is to reduce the local volume fraction on the top surface.

5. Summary

In summary, we treat an individual CNT as a roll of graphite and numerically studied the effect of various randomness and obliqueness of the CNT arrays. In terms of reflection, the random position, diameter, and random small inclination arrays are all quite similar to the ordered array, while the random length array can largely suppress the reflectance. Arrays of MWCNT with randomness in position and length have similar absorptance as the ordered array. Random diameter and random small inclination angle cause slight enhancement in absorption as compared to ordered arrays. Compared to silicon nanowire arrays, the optical property of vertically aligned CNTs is not as sensitive to structural randomness. The inclination of CNT array shows strong angular dependence for S-polarized light due to the anisotropic nature of CNTs, while for P-polarized light the dependence is small. We have also shown that large inclination angle has a strong effect on the reflectance of CNTs, primarily due to the increase of local volume fraction on the top surface. Therefore, to experimentally achieve better blackbody absorbers, further efforts should be devoted to reducing the local volume fraction of the top surface.

Acknowledgments

This work was partly supported by the Air Force Office of Scientific Research through the Discovery Challenge Thrust (DCT) Program (Grants no. FA9550-08-1-0126 and FA9550-11-1-0057, Program Managers Dr. Kumar Jata and Dr. Joan Fuller). HB also acknowledges the support of the startup fund from Shanghai Jiao Tong University.

References

[1] Iijima S. Nature 1991;354:56.
[2] Kempa K, Ryhczynski J, Huang ZP, Gregorczyk K, Vidan A, Kimball B, et al. Adv Mater 2007;19:421.
[3] Bychanok D, Kanygin M, Okotrub A, Shuba M, Paddubskaya A, Pliushch A, et al. JETP Lett 2011;93:607.
[4] Yang Z-P, Ci L, Bur JA, Lin S-Y, Ajayan PM. Nano Lett 2008;8:446.
[5] Wang XJ, Flicker JD, Lee BJ, Ready WJ, Zhang ZM. Nanotechnology 2009;20:215704.
[6] Mizuno K, Ishii J, Kishida H, Hayamizu Y, Yasuda S, Futaba DN, et al. Proc Natl Acad Sci 2009;106:6044.
[7] Wang XJ, Wang LP, Adewuyi OS, Cola BA, Zhang ZM. Appl Phys Lett 2010;97:163116.
[8] Zhang ZM, Tsai BK, Machin G. Radiometric temperature measurements: II&I. New York: Academic; 2010.
[9] Fainchtein R, Brown DM, Siegrist KM, Monica AH, Hwang E, Milner SD, et al. Phys Rev B 2012;85:125432.
[10] Guo GY, Chu KC, Wang DS, Duan CG. Phys Rev B 2004;69:205416.
[11] Sisto A. Master's thesis. West Lafayette, IN: Purdue University; 2011.
[12] Lidorikis E, Ferrari AC. ACS Nano 2009;3:1238.
[13] Bao H, Ruan XL, Fisher TS. Opt Express 2010;18:6347.
[14] Bao H, Ruan XL. Opt Lett 2010;35:3378.
[15] Li J, Yu H, Wong SM, Zhang G, Sun X, Lo PG, Kwong D. Appl Phys Lett 2009;95:033102.
[16] Lin C, Povinelli ML. Opt Express 2009;17:19371.
[17] Fan Z, Kapaida R, Leu PW, Zhang X, Chueh Y, Takei K, et al. Nano Lett 2010;10:3823.
[18] Zhu J, Yu Z, Burkhard GF, Hsu CM, Connor ST, Xu Y, et al. Nano Lett 2009;9:279.
[19] Botello-Méndez A, Campos-Delgado J, Morelos-Gómez A, Romo-Herrera H, Rodríguez AG, Navarro H, et al. Chem Phys Lett 2008;453:55.